Trans. Japan Soc. Aero. Space Sci.
Vol. 62, No. 2, pp. 86–92, 2019
DOI: 10.2322/tjsass.62.86

Radiative Characteristics of N_2 First Positive Band in Visible and Near-infrared Regions for Microwave-discharged Nitrogen Plasma*

Kenji SHIBUSAWA[1)†] and Masato FUNATSU[2)]

[1)]*Department of Industrial Engineering, National Institute of Technology, Ibaraki College, Hitachinaka, Ibaraki 312–8508, Japan*
[2)]*Graduate School of Science and Technology, Gunma University, Kiryu, Gunma 376–8515, Japan*

The spectroscopic measurement of low-pressure microwave-discharged nitrogen plasma was conducted in the wavelength region of 550 to 1070 nm. Radiation from the N_2 first positive band of the $\Delta v = 0$ to $\Delta v = +4$ band series and nitrogen atomic lines were observed. The experimental spectrum was compared with the theoretical spectrum, showing the effect of the predissociation of N_2 B $^3\Pi_g$ state through N_2 A′ $^5\Sigma_g{}^+$ state and triplet splitting for the transition of $^3\Pi$ to the $^3\Sigma$ state. They agreed very well with each other for the $\Delta v = 0$ to $\Delta v = +2$ band series, which consisted of the lower vibrational levels of $v' = 0$ to 7, but did not agree well for the higher vibrational levels of $v' = 8$ to 12 in the $\Delta v = +3$ and $+4$ band series. By comparing the band head intensity of the experimental and theoretical spectra, the experimental vibrational population on each vibrational level for the B $^3\Pi_g$ state was estimated to be a non-Boltzmann distribution at the higher vibrational levels. In addition, the theoretical vibrational population distribution in the B $^3\Pi_g$ state was calculated using a master equation, and then agreement between the experimental spectrum and the theoretical spectrum with the non-Boltzmann distribution obtained from the master equation was improved.

Key Words: Plasma, Radiation, Spectroscopic Measurement, Microwave Discharge, Vibrational Nonequilibrium

Nomenclature

$A(v', v'')$: sum of radiative transition probability from vibrational level v' in B $^3\Pi_g$ state to all vibrational levels in A $^3\Sigma_u{}^+$ state
$K(c, v')$: recombination rate coefficient to vibrational level of v'
$K(v', c)$: dissociation rate coefficient from vibrational level of v'
$K(v, v')$: transition rate coefficient from an initial level v in B $^3\Pi_g$ state to final level v'
J_{max}: maximum rotational quantum number
n_M: population of third body
n_S: population in $^4S°$ state of nitrogen atom
$n_{v'}$: population of vibrational level v'
T_r: rotational temperature
T_v: vibrational temperature
v': vibrational level in B $^3\Pi_g$ state
v'': vibrational level in A $^3\Sigma_u{}^+$ state
Δv: $v' - v''$
V_{max}: maximum vibrational quantum number
λ_D: surprisal parameter for dissociation

1. Introduction

Spectroscopic measurement has been conducted for arc-heated wind tunnels,[1,2)] shock tubes,[3)] and inductively coupled plasma[4)] to determine the physical properties of high-temperature plasma. Since it is frequently used for temperature determination by comparing with theoretical spectrum, it is important to improve the accuracy of the theoretical spectrum and to understand the internal state of a molecule or an atom concerned with the occurrence of the spectrum. In general, the radiation from $N_2{}^+$, N_2, and N is often observed when using nitrogen gas as a test gas. In the ultraviolet region, radiation of the N_2 second positive (2+) band and $N_2{}^+$ first negative (1−) band is mainly observed, and the radiation is strong. In the visible and near-infrared regions, the N_2 first positive (1+) band is also often observed, but the radiation is normally weaker than that of the N_2 2+ band. The N_2 1+ band has been intensively investigated for afterglow plasma.[5,6)] The N_2 1+ band originates from the radiative transition of N_2 B $^3\Pi_g$ to the N_2 A $^3\Sigma_u{}^+$ state, and the B $^3\Pi_g$ state is well known as having a predissociation process through the A′ $^5\Sigma_g{}^+$ state. This process significantly affects occurrence of the N_2 1+ band. Furthermore, it is difficult to observe the A′ $^5\Sigma_g{}^+$ state directly, and this state contributes not only to the dissociation and recombination process in a nitrogen plasma, but also produces a metastable state.[6)] Therefore, to understand the processes concerned with the B $^3\Pi_g$ and A′ $^5\Sigma_g{}^+$ states precisely, it is important to predict the properties of the recombining plasma and nonequilibrium plasma more accurately.

In the present study, in order to obtain the N_2 1+ band, nitrogen plasma was generated by a microwave discharge at a low pressure and spectroscopic measurement was conducted. A microwave discharge enables us to relatively easily obtain nonequilibrium plasma, and the N_2 2+ band was observed clearly in the ultraviolet region.[7)] To sustain stable plasma easily and investigate the nonequilibrium using the condition

*Presented at the 28th International Symposium on Space Technology and Science, 5–12 June 2011, Okinawa, Japan.
Received 8 September 2017; final revision received 28 August 2018; accepted for publication 16 October 2018.
†Corresponding author, shibusawa@mech.ibaraki-ct.ac.jp

where it was observed, plasma was generated at the pressure of 700 Pa and incident power of 200 W. In general, the N_2 1+ band has mainly been observed in the visible region. However, we can only obtain radiation from a vibrational level of more than $v' = 2$ in the visible region. In this study, in order to observe radiation from the ground vibrational level in the near-infrared region, and to investigate the radiative characteristics with a sufficiently high intensity for the long-wavelength region, spectroscopic measurement was conducted using a near-infrared photomultiplier tube and a photon counting system. This experimental setup enabled us to observe the N_2 1+ band along with a wide wavelength region and obtain the radiation from all vibrational levels up to 12. In this experiment, spectroscopic measurement of the microwave-discharged nitrogen plasma was conducted in the wavelength region from 550 to 1070 nm. The radiative intensity observed during the experiment was compared with the theoretical spectrum for the N_2 1+ band. From the results, since the experimental spectrum with higher vibrational levels was not reconstructed using the theoretical spectrum with Boltzmann equilibrium, the vibrational population distribution in the N_2 B $^3\Pi_g$ state was numerically calculated using a master equation. The master equation is often applied to investigate rotational and vibrational relaxation for high-temperature plasma and nonequilibrium plasma.[8–10] In the analysis, the model of rate coefficients for excitation and dissociation is important, and was developed for vibrational energy transfer[8] and rotational energy transfer, individually. Recently, studies for developing rotational and vibrational master equations have begun, and defined rate coefficients have been verified by making comparisons with previous models or shock tube experiments.[9,10]

In our experiment, vibrational nonequilibrium in the N_2 B $^3\Pi_g$ state was measured by comparing the experimental spectrum and theoretical spectrum, but rotational nonequilibrium could not be confirmed due to the complicated rotational lines on each band head. Hence, we estimated the vibrational population at the N_2 B $^3\Pi_g$ state by calculating the vibrational master equation. In the calculation, the vibrational transition rate coefficient based on information theory[11] and the modified model of the dissociation rate coefficient of Gonzales and Varghese,[12] as mentioned by Sakamura,[13] were considered. Using the non-Boltzmann population distribution obtained from the master equation, the vibrational nonequilibrium in the N_2 B $^3\Pi_g$ state was investigated, and improving the theoretical spectrum for the N_2 1+ band was attempted.

2. Experimental Setup

Figure 1 shows a schematic view of the experimental setup. The microwave-generating system is composed of a microwave generator, isolator, power monitor, EH tuner, and rectangular cavity resonator. A quartz tube with an inside diameter of 10 mm was inserted into the aperture of the cavity resonator. Nitrogen gas was forced to flow in the tube with a constant flow rate of 50 ml/min, and was exhausted by an oil-rotary pump. Then the pressure in the tube was kept at 700 Pa. The microwave at a frequency of 2.45 GHz was transmitted into the cavity, and microwave-discharged nitrogen plasma was generated under the incident power of 200 W. Figure 2 shows a schematic view of the measuring point. The length of the plasma generated was about 55 mm and it was very steady. The spectroscopic measurement was conducted at a position of 30 mm from the upstream end of the cavity on the center axis. Radiation from the plasma was measured by a spectrometer (Andor SR500) with a grating of 1200 grooves/mm and a focal distance of 500 mm using a near-infrared photomultiplier tube (Hamamatsu Photonics R5509-43) and a photon counting system (Hamamatsu Photonics C9744 and C8855-01). An achromatic lens with an applicable range of 500 to 1100 nm was used not only to focus on the radiation of the plasma on the entrance slit of the spectrometer, but also for preventing chromatic aberration. In this experiment, a spectrum over the wide wavelength region of 550 to 1070 nm was measured in order to obtain as much of the N_2 1+ band series as possible. A longpass filter was also set in front of the entrance slit to eliminate a secondary spectrum in the shorter-wavelength region of 550 nm. After measuring the spectrum, the sensitivity profile depending on wavelength for the measuring system was calibrated using a calibrated 200 W tungsten halogen source lamp (Newport 63355).

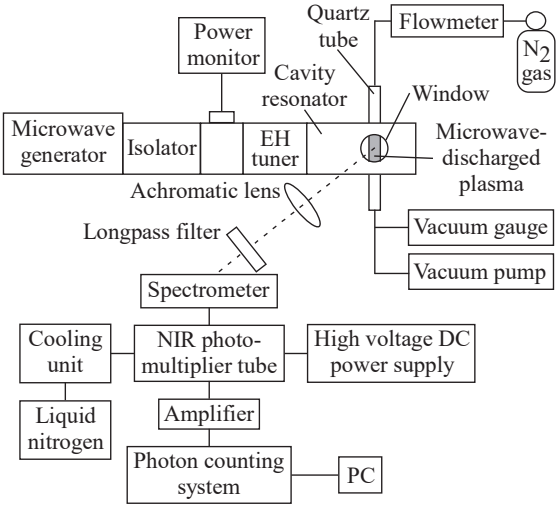

Fig. 1. Schematic view of experimental setup.

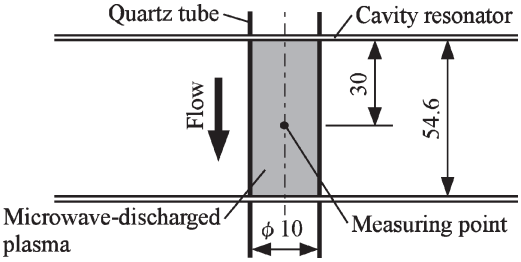

Fig. 2. Schematic view of measuring point.

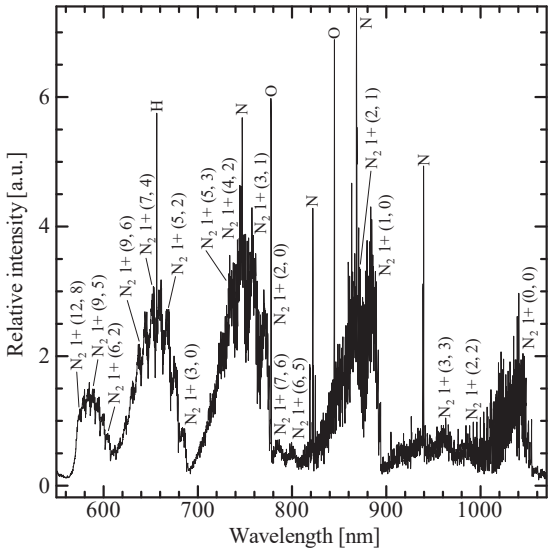

Fig. 3. Experimental spectrum.

3. Radiative Characteristics of N_2 1+ Band

3.1. Experimental spectrum

Figure 3 shows the experimental spectrum between 550 and 1070 nm. The experimental spectrum was normalized using the intensity of the N_2 1+ (0, 0) band at 1051 nm. It is mainly composed of the N_2 1+ band for the $\Delta v = 0$ to $\Delta v = +4$ band series and some atomic lines. The H and O lines are contamination in the gas. In each band series of the N_2 1+ band, the band heads for some upper vibrational levels are distinguishable. In the near-infrared region, the radiation from a ground vibrational energy level in the B $^3\Pi_g$ state was clearly observed, and the rotational lines could be identified more sharply. In the $\Delta v = +3$ and $+4$ band series, the radiation from the higher vibrational energy levels more than $v' = 7$ could be observed. The radiation from $v' > 12$ was observed in the Lewis-Rayleigh afterglow[5] at lower pressure, but it was not obviously distinguished in this experiment. The upper vibrational level in the B $^3\Pi_g$ state for distinguishable band heads in each band series is tabulated in Table 1. The band heads in parentheses in this table are overlapped in the same wavelength region. Similarly, the radiation from a higher vibrational level in the $\Delta v = 0$ to $\Delta v = +2$ band series are overlapped with other band series. Therefore, to understand the radiative characteristics from all vibrational levels in the B $^3\Pi_g$ state, it is necessary to measure the spectrum along with a wide wavelength region.

3.2. Theoretical spectrum of N_2 1+ band

In order to investigate the radiative characteristics of the N_2 1+ band in detail, a theoretical spectrum for the N_2 1+ band was calculated. In the calculation, the theoretical spectrum was constructed based on line-by-line calculation.[14] Since the origin of the N_2 1+ band is radiative transition from N_2 B $^3\Pi_g$ to the N_2 A $^3\Sigma_u{}^+$ state, triplet splitting for the transition from $^3\Pi$ to $^3\Sigma$ was considered, and then 27 branches were included.[15] The B $^3\Pi_g$ state is known to interact with the N_2 A$'$ $^5\Sigma_g{}^+$ state, and it is indicated that a predissociation limit exists near 9.99 eV at $v = 12$ and $j = 33$.[16] Figure 4 shows the potential curves for the B $^3\Pi_g$ and A$'$ $^5\Sigma_g{}^+$ states of N_2. These curves were calculated by combining the Rydberg-Klein-Rees and Hulburt-Hirschfelder methods[17] using the spectroscopic data.[18,19] The two curves for the B $^3\Pi_g$ and A$'$ $^5\Sigma_g{}^+$ states cross above the vibrational level of 10 in the B $^3\Pi_g$ state, as shown in this figure, and the N_2 B $^3\Pi_g$ molecule having the energy above the predissociation limit is dissociated through the A$'$ $^5\Sigma_g{}^+$ state to two nitrogen atoms with a ground-level $^4S^\circ$ state. Originally, the B $^3\Pi_g$ state has a vibrational level of 30 and much higher rotational levels on each vibrational level. However, the predissociation process eliminates the radiation from $v' > 12$ and higher rotational levels, and a unique spectrum of the N_2 1+ band is formed. Therefore, in this calculation, the radiation from the B $^3\Pi_g$ state above the energy level on $v = 12$ and $j = 33$ was eliminated, and the maximum rotational quantum number J_{max} for each vibrational level was determined from the predissociation energy of the B $^3\Pi_g$ state.

Table 1. Vibrational level on B $^3\Pi_g$ state for distinguishable band heads in each band series.

	Vibrational level on B $^3\Pi_g$ state
$\Delta v = 0$	0 2 3 4 5
$\Delta v = +1$	1 2 3 6 7
$\Delta v = +2$	2 3 4 5 6 7
$\Delta v = +3$	3 4 5 6 7 8 9 10 11 (12)
$\Delta v = +4$	(4) 5 6 7 8 9 10 11 12

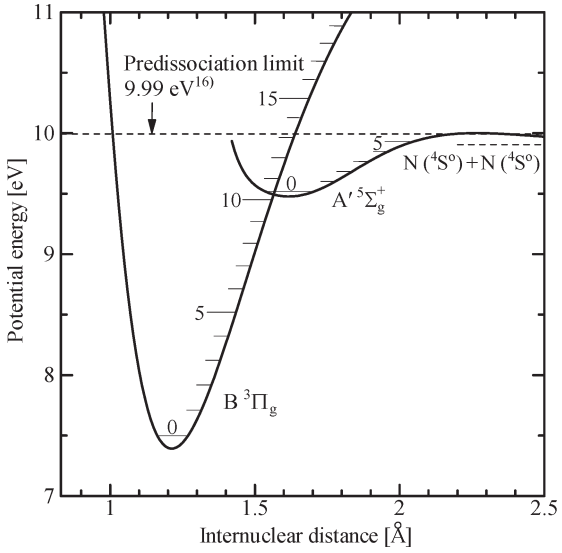

Fig. 4. Potential curves for B $^3\Pi_g$ and A$'$ $^5\Sigma_g{}^+$ states of N_2.

Figure 5 shows a comparison between the theoretical spectrum with the effect of predissociation and the theoretical spectrum without the effect of predissociation. The former was calculated using a maximum vibrational quantum number of $V_{max} = 12$, and the latter was calculated using $V_{max} = 21$ owing to restricting the data[18] for Franck-Condon factor, radiative transition probability, and so on. The vibrational and rotational population distributions were as-

sumed to be Boltzmann distributions, and the theoretical spectra were calculated for a vibrational temperature of 7500 K and a rotational temperature of 6500 K. In this figure, both spectra were normalized using the intensity of the N_2 1+ (0, 0) band at 1051 nm. The spectra for the $\Delta v = +2$ band series composed from lower vibrational levels of $v' = 0$ to 7 had nearly the same profiles. But in the $\Delta v = +3$ to +5 band series, the intensity from higher vibrational levels for the spectrum without predissociation gradually became higher than the spectrum with predissociation. Especially, the radiation from the vibrational levels of more than 13 dramatically changed. Since the radiation for $v' > 12$ was not observed in this experiment, as shown in Fig. 3, it was found that consideration of the predissociation for the B $^3\Pi_g$ state through A$'$ $^5\Sigma_g{}^+$ state is necessary and very important for precise reconstruction of the N_2 1+ band.

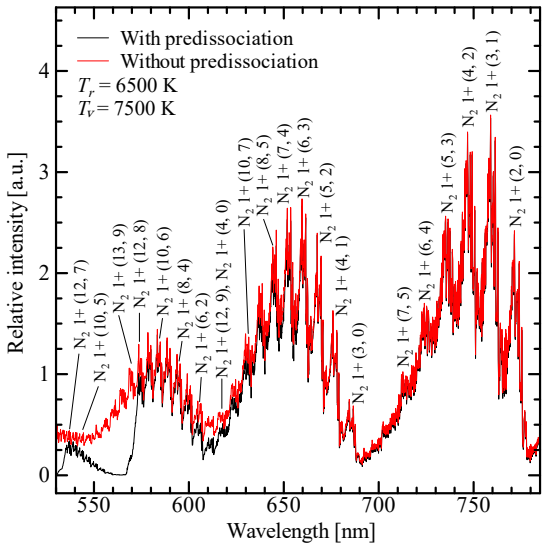

Fig. 5. Comparison of theoretical spectra.

3.3. Comparison of experimental and theoretical spectra

The theoretical spectrum with the effect of the predissociation shown in Fig. 5 was compared with the experimental spectrum. Figure 6 shows a comparison of the experimental spectrum and theoretical spectrum calculated at the temperatures of $T_r = 6500$ K and $T_v = 7500$ K. In the present study, temperature determination was conducted by applying the spectral matching method. As vibrational temperature increases, the intensity of the band head with higher levels of vibration in the upper state becomes relatively higher. As rotational temperature increases, the intensity in the shorter-wavelength region of each band head becomes relatively higher. We estimated the vibrational temperature from the ratio of each band head intensity and the rotational temperature from the shape of the slope in the shorter-wavelength region of each band series by comparing the appearance of the experimental spectrum and theoretical spectra for several temperature conditions. The vibrational temperature was higher than the rotational temperature. Then, the microwave-discharged nitrogen plasma was estimated to be in a thermal nonequilibrium state.

From Fig. 6, it was found that the theoretical spectrum agreed well with the experimental spectrum for the entire wavelength region to some extent, but agreement was inadequate for bands with higher levels of vibration in the B $^3\Pi_g$ state. A detailed comparison of the experimental spectrum and theoretical spectrum for the $\Delta v = 0$ band series is shown in Fig. 7(a) and that for the $\Delta v = +4$ band series in Fig. 7(b). In the $\Delta v = 0$ band series, though the intensity of each rotational line of the N_2 1+ band was not precisely reconstructed and the atomic lines were not included in the theoretical spectrum, both spectra were in good agreement. On the other hand, in the $\Delta v = +4$ band series, the intensity of the theoretical spectrum in the wavelength region less than the N_2 1+ (7, 3) band gradually rose higher than that in the experimental spectrum. This fact indicated that the vibrational population distribution in the B $^3\Pi_g$ state with higher

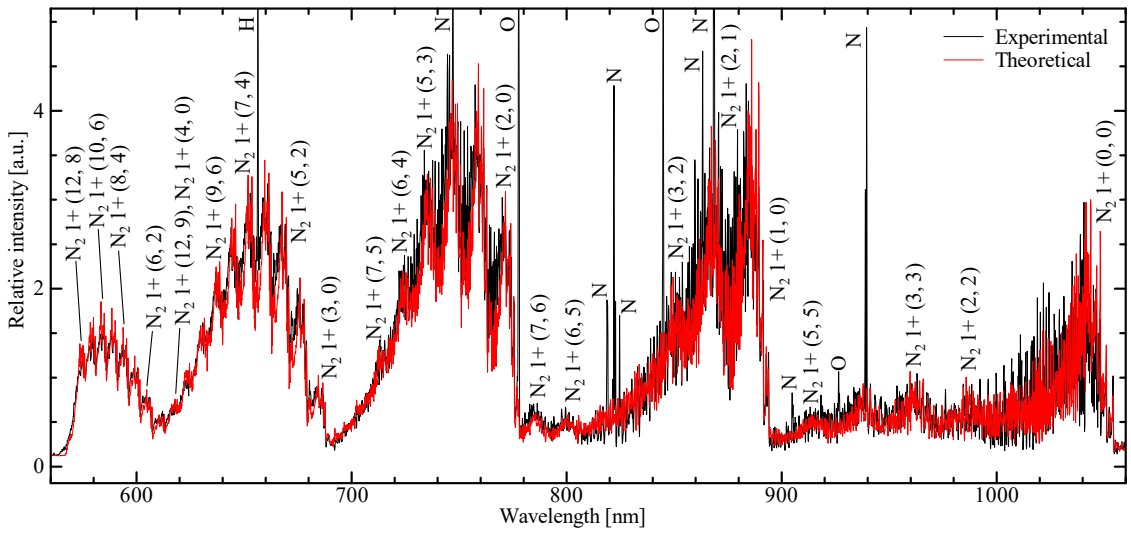

Fig. 6. Comparison of experimental and theoretical spectra.

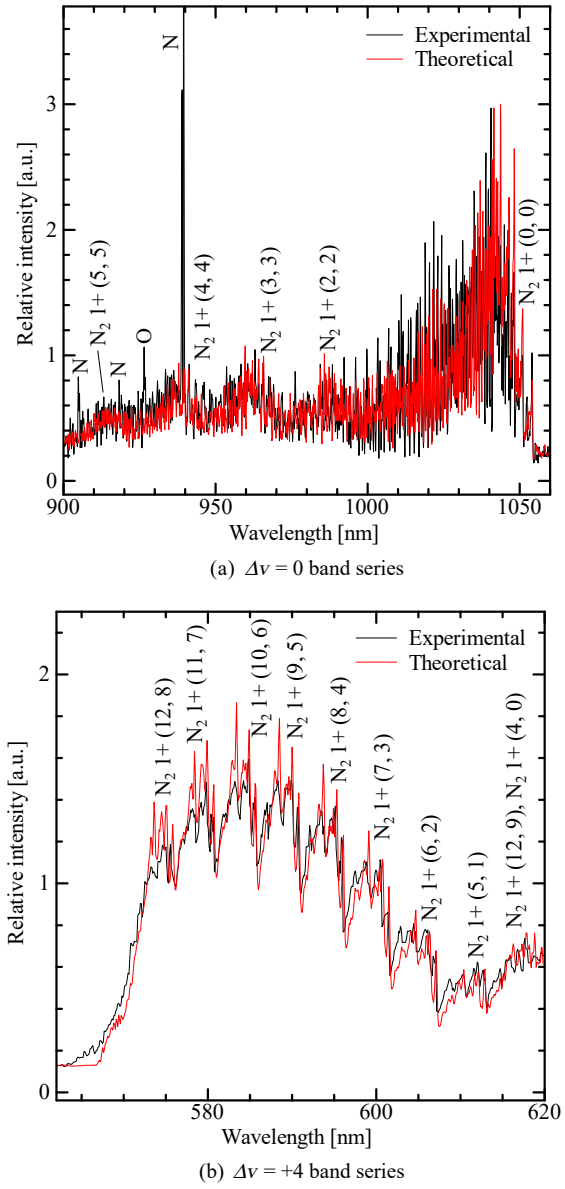

(a) $\Delta v = 0$ band series

(b) $\Delta v = +4$ band series

Fig. 7. Comparison of experimental and theoretical spectra in each band series.

levels of vibration was not in Boltzmann equilibrium. In this study, in order to investigate vibrational nonequilibrium, the vibrational population in the N_2 B $^3\Pi_g$ state was analyzed numerically using a master equation.

4. Analysis of Vibrational Population Distribution

4.1. Master equation

In the present study, a master equation was used to calculate the vibrational population in the N_2 B $^3\Pi_g$ state for which the vibrational level was 13; that is, $v' = 0$ to $v' = 12$. In the equation, the effects of vibrational transition, dissociation, and recombination resulting from heavy particle collisions, and also the radiative transition from the N_2 B $^3\Pi_g$ state to the N_2 A $^3\Sigma_u^+$ state were included. The master equation is described in the following form,

$$\frac{dn_{v'}}{dt} = \sum_{v' \neq v} \left[K(v, v')n_v n_M - K(v', v)n_{v'} n_M \right] - K(v', c)n_{v'} n_M + K(c, v')n_S{}^2 n_M - A(v', v'')n_{v'}, \quad (1)$$

where, the lefthand-side of Eq. (1) indicates the rate of change in the population on the vibrational level v'. On the righthand-side, the first term indicates the change in rate of the population resulting from vibrational transition due to heavy particle collision; the second term represents change due to dissociation from vibrational level v', and the third and fourth terms represent change due to recombination and radiative transition from the B $^3\Pi_g$ to A $^3\Sigma_u^+$ states, respectively. For this calculation, we assumed the dissociation and recombination occurred directly between the B $^3\Pi_g$ state and $^4S^\circ$ state of the nitrogen atom, without considering predissociation through the A′ $^5\Sigma_g^+$ state.

In this study, the vibrational de-excitation transition rate coefficient $K(v', v)$ derived applying the information theory[11] and modified model[13] of the dissociation rate coefficient $K(v', c)$ originally derived from Gonzales and Varghese[12] were used. The excitation rate coefficient and recombination rate coefficient were derived applying the principle of detailed balance. In order to estimate the effects among vibrational transition, dissociation, and radiative transition, the coefficients of n_v on the righthand-side of Eq. (1) were calculated under the experimental conditions of a pressure of 700 Pa and a vibrational temperature of 7500 K. Representing the total change in the population rate on vibrational level v' using vibrational transition as K_{trans}, giving dissociation as K_{dis} and radiative transition as K_{rad}, these terms are described in the following forms,

$$K_{trans} = \sum_{v' \neq v} K(v', v)n_M, \quad (2)$$

$$K_{dis} = K(v', c)n_M, \quad (3)$$

$$K_{rad} = A(v', v''). \quad (4)$$

The comparison of Eqs. (2), (3), and (4) is shown in Fig. 8. For the plasma conditions considered here, the total change rates due to vibrational transition and due to radiative transition can be determined uniquely, but the change rate due to dissociation is adjustable applying the surprisal parameter λ_D.[12] In this figure, the total change rates due to dissociation for $\lambda_D = 10$, 25, and 50 are shown. The total change rate resulting from vibrational transition is larger than other rates and the effect of radiative transition is negligible. However, it can be seen that the difference between the rates due to vibrational transition and dissociation becomes considerably smaller as the vibrational level rises, and the value of λ_D decreases. For the lower value of λ_D, one can predict that the effect of dissociation will appear relatively easily in the population distribution obtained from the master equation.

4.2. Theoretical vibrational population distribution

Theoretical vibrational population distribution in the N_2 B $^3\Pi_g$ state was calculated using the master equation. It was as-

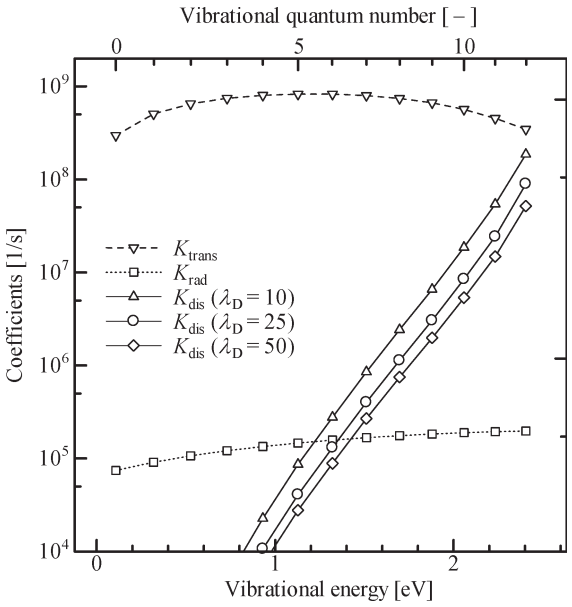

Fig. 8. Comparison of coefficients among K_{trans}, K_{dis}, and K_{rad}.

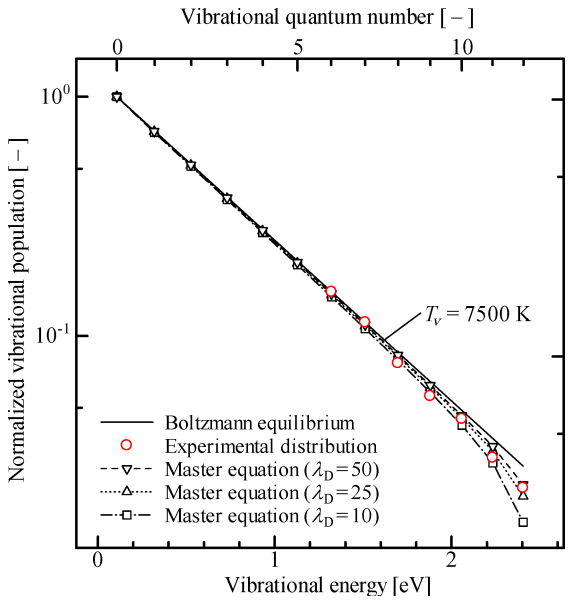

Fig. 9. Vibrational population distributions.

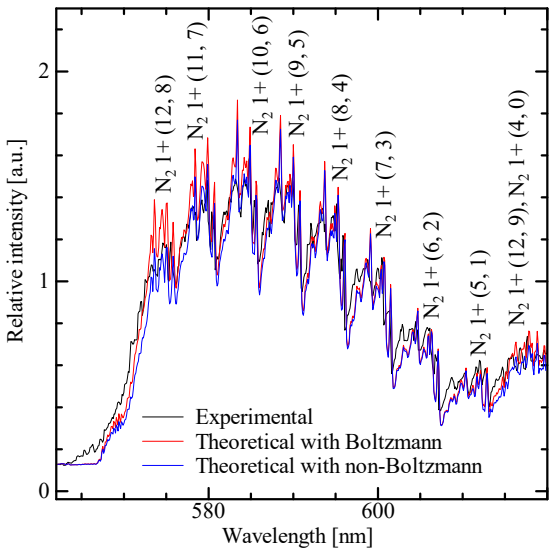

Fig. 10. Comparison of experimental spectrum, theoretical spectrum with Boltzmann equilibrium, and theoretical spectrum with non-Boltzmann vibrational population distribution.

sumed that the plasma was in the steady state corresponding to the experiment. Thus, numerically solving the 13×13 matrix generated from the master equation with $dn_{v'}/dt = 0$, the population at each vibrational level was obtained. In this calculation, the temperature was assumed to be 7500 K and the pressure was 700 Pa, the same as the experiment. Figure 9 shows a comparison of the theoretical vibrational population distributions for $\lambda_D = 10$, 25, and 50. The horizontal axis is the vibrational energy and the vertical axis is the normalized vibrational population. The population at each vibrational level was normalized using the value of the population at the ground vibrational level. From the results, it was found that the vibrational population distribution obtained from the master equation formed a non-Boltzmann distribution. As the value of λ_D becomes lower, the decline in population at higher vibrational levels becomes larger. In Fig. 9, the experimental vibrational population distribution estimated from the $\Delta v = +4$ band series so as to fit each band head intensity of the experimental spectrum by adjusting the population on each vibrational level of the theoretical spectrum was also plotted. The population was normalized using the population value at $v' = 6$ so as to agree with Boltzmann distribution because the vibrational populations at the lower vibrational levels up to 6 were thought to be within Boltzmann equilibrium. From this figure, in the case of $\lambda_D = 25$, it was found that the tendency of the experimental vibrational population distribution was relatively well reconstructed.

Figure 10 shows a comparison of the experimental spectrum and the theoretical spectrum with the non-Boltzmann population distribution calculated using the master equation for $\lambda_D = 25$ in the $\Delta v = +4$ band series. By considering the non-Boltzmann population distribution, agreement between the experimental and theoretical spectra was improved. Therefore, it is important to consider the non-Boltzmann vibrational population distribution for the theoretical spectra to reconstruct the experimental spectra precisely. However, the intensity of the theoretical spectrum in a shorter-wavelength region on each band was somewhat smaller than the experimental spectrum. This tendency was also seen in other band series. One possible reason is thought to be in the accuracy of the Hönl-London factor. Moreover, the intensity of the theoretical spectrum was lower than that of the experimental spectrum in the shorter-wavelength region of the N_2 1+ (12, 8) band. Since the theoretical spectrum including the vibrational levels of $v' = 13$ and 14 did not reconstruct the slope of the experimental spectrum, another possible reason is thought to be overlapping with other bands from N_2 2+, N_2^+ 1− or N_2 1+ of $v' > 17$ observed in the Lewis-Rayleigh afterglow.[20] Consideration of details will be needed in the future. Concerning the surprisal parameter, Gonzales

and Varghese estimated the value to be approximately $\lambda_D = 1$ for N_2 from the comparison using shock tube data.[12] The vibrational population for $\lambda_D = 1$, calculated from the master equations, became much lower than the population of the experimental distribution in Fig. 9. In this study, we assumed the direct occurrence of dissociation and recombination without considering predissociation, and calculation was carried out using the master equation. Considering predissociation and other processes for the N_2 B $^3\Pi_g$ state are required for the master equation.

5. Conclusion

Spectroscopic measurement of the microwave-discharged nitrogen plasma at low pressure was conducted in the wavelength region of 550 to 1070 nm and the N_2 1+ band from the $\Delta v = 0$ to $\Delta v = +4$ band series was observed. In the $\Delta v = 0$ band series of the near-infrared region, radiation from the ground vibrational energy level was clearly observed. In the $\Delta v = 0$ to $\Delta v = +2$ band series, radiation from the vibrational levels up to 7 in the B $^3\Pi_g$ state was observed. It was found that the experimental spectrum for the lower vibrational levels was well reconstructed using the theoretical spectrum with Boltzmann equilibrium. However, the experimental spectrum with higher vibrational levels up to 12 in the $\Delta v = +4$ band series was not fitted to the theoretical spectrum with Boltzmann equilibrium. From the results, it was found that the population in the B $^3\Pi_g$ state with higher levels of vibration was relatively small compared to the Boltzmann distribution. In this study, the vibrational population distribution in the B $^3\Pi_g$ state was calculated using the master equation, and non-Boltzmann distributions were obtained depending on the value of the surprisal parameter λ_D. The theoretical spectrum with non-Boltzmann distribution for $\lambda_D = 25$ agreed well with the experimental spectrum. However, consideration for predissociation of the B $^3\Pi_g$ state through the A′ $^5\Sigma_g^+$ state was not directly included in this master equation calculation. The effect of predissociation needs to be included in the calculation in the future.

Acknowledgments

This work was supported by Grant-in-Aid for Young Scientists (B) (No. 21760657) of the Japan Society for the Promotion of Science.

References

1) Park, C. S., Newfield, M. E., Fletcher, D. G., and Gökçen, T.: Spectroscopic Measurements of the Flows in an Arc-jet Facility, AIAA Paper 98-0893, 1998.
2) Winter, M. W., Prabhu, D. K., Raiche, G. A., Terrazas-Salinas, I., and Hui, F. C. L.: Emission Spectroscopic Measurements with an Optical Probe in the NASA Ames IHF Arc Jet Facility, AIAA Paper 2012-1016, 2012.
3) Sharma, S. P. and Gillespie, W.: Nonequilibrium and Equilibrium Shock Front Radiation Measurements, AIAA Paper 90-0139, 1990.
4) Fujita, K., Mizuno, M., Ishida, K., Ito, T., Sumi, T., and Kurotaki, T.: Spectroscopic Diagnostics of Electrically Heated High Enthalpy Wind Tunnels, AIAA Paper 2005-173, 2005.
5) Becker, K. H., Fink, E. H., Groth, W., Jud, W., and Kley, D.: N_2 Formation in the Lewis-Rayleigh Afterglow, *Faraday Discuss. Chem. Soc.*, **53** (1972), pp. 35–51.
6) Partridge, H., Langhoff, S. R., Bauschlicher, C. W., Jr., and Schwenke, D. W.: Theoretical Study of the A′ $^5\Sigma_g^+$ and C″ $^5\Pi_u$ States of N_2: Implications for the N_2 Afterglow, *J. Chem. Phys.*, **88** (1988), pp. 3174–3186.
7) Shibusawa, K., Funatsu, M., Shirai, H., and Takakusagi, F.: Radiation and Temperature Characteristics of N_2 Second Positive Bands of Microwave-discharged Plasmas at Low Pressure, *J. Jpn. Soc. Aeronaut. Space Sci.*, **55** (2007), pp. 232–238 (in Japanese).
8) Capitelli, M., Colonna, G., D'Ammando, G., Laporta, V., and Laricchiuta, A.: Nonequilibrium Dissociation Mechanisms in Low Temperature Nitrogen and Carbon Monoxide Plasmas, *Chem. Phys.*, **438** (2014), pp. 31–36.
9) Kim, J. G. and Boyd, I. D.: State-resolved Master Equation Analysis of Thermochemical Nonequilibrium of Nitrogen, *Chem. Phys.*, **415** (2013), pp. 237–246.
10) Panesi, M., Jaffe, R. L., Schwenke, D. W., and Magin, T. E.: Rovibrational Internal Energy Transfer and Dissociation of N_2 ($^1\Sigma_g^+$)–N (^4S_u) System in Hypersonic Flows, *J. Chem. Phys.*, **138** (2013), 044312.
11) Procaccia, I. and Levine, R. D.: Vibrational Energy Transfer in Molecular Collisions: An Information Theoretic Analysis and Synthesis, *J. Chem. Phys.*, **63** (1975), pp. 4261–4279.
12) Gonzales, D. A. and Varghese, P. L.: Evaluation of Simple Rate Expressions for Vibration-dissociation Coupling, *J. Thermophys. Heat Trans.*, **8** (1994), pp. 236–243.
13) Sakamura, Y.: A Master Equation Study of Vibration-dissociation Coupling in Shock-heated Oxygen Molecules, *Shock Waves*, **12** (2003), pp. 361–373.
14) Arnold, J. O., Whiting, E. E., and Lyle, G. C.: Line by Line Calculation of Spectra from Diatomic Molecules and Atoms Assuming a Voigt Line Profile, *J. Quant. Spectrosc. Radiat. Transfer.*, **9** (1969), pp. 775–798.
15) Budó, A.: Intensitätsformeln für die Triplettbanden, *Z. Physik*, **105** (1937), pp. 579–587.
16) Vanderslice, J. T., Mason, E. A., and Lippincott, E. R.: Interactions between Ground-state Nitrogen Atoms and Molecules. The N-N, N-N_2, and N_2-N_2 Interactions, *J. Chem. Phys.*, **30**, 1 (1959), pp. 129–136.
17) Vanderslice, J. T., Mason, E. A., and Maisch, W. G.: Interactions between Oxygen and Nitrogen: O-N, O-N_2, and O_2-N_2, *J. Chem. Phys.*, **31**, 3 (1959), pp. 738–746.
18) Laux, C. O.: Optical Diagnostics and Radiative Emission of Air Plasmas, HTGL Report, Stanford University Ph.D. Thesis, T-288, 1993.
19) Park, C.: *Nonequilibrium Hypersonic Aerothermodynamics*, John Wiley and Sons, New York, 1990.
20) Ung, A. Y.-M.: Observations of the High Vibrational Levels of N_2 (B $^3\Pi_g$) in the Lewis-Rayleigh Afterglow of Nitrogen, *J. Chem. Phys.*, **65** (1976), pp. 2987–2990.

Naofumi Ohnishi
Associate Editor